Bulletin of Earthquake Engineering
https://doi.org/10.1007/s10518-022-01405-z

ORIGINAL ARTICLE

Pin-supported walls as seismic retrofit for existing RC frames: feasibility and preliminary design

Elena Casprini[1] · Andrea Belleri[1] · Alessandra Marini[1] · Simone Labò[1] · Chiara Passoni[1]

Received: 13 August 2021 / Accepted: 8 April 2022

Abstract
The seismic retrofit of the existing building heritage represents an urgent issue to be faced and innovative solutions which allow to overcome renovation barriers are needed. In this scenario, pin-supported (PS) walls represent an eligible solution, enabling linearization of the deformation of the frame along its height and inhibiting soft storey collapse mechanisms. The PS wall can be connected to the existing building from outside, thereby avoiding disruption to occupants or their relocation, which are acknowledged as the main barriers to the renovation nowadays. Suitability of PS wall solutions in the seismic retrofit of the existing building stock has been investigated herein, particularly in the case of existing reinforced concrete (RC) buildings, preliminarily focusing on 2D RC frames. The paper shows the weaknesses and strengths of the PS wall solution in relation to the specific features of the considered buildings. An analytical closed-form formulation is proposed and applied as a preliminary tool to evaluate the load distribution in the existing frame and in the PS wall after the retrofit considering the first mode of vibration of the retrofitted system. The results show that, in some conditions, the application of PS walls may be detrimental to the structural response. Along with the evaluation of the effectiveness of the retrofit solution, the proposed formulation allows a preliminary design of the retrofit system. Finally, a series of finite element model analyses have been carried out for validation purposes showing a good agreement between the proposed analytical formulation and the numerical results.

Keywords Pin-supported walls · Hinged walls · Rocking cores · Seismic retrofit · RC buildings · RC frames

1 Introduction

Most of the existing European buildings are vulnerable to seismic actions, particularly those buildings designed before the enforcement of modern anti-seismic regulations and seismic zonation; the post-Second World War reinforced concrete (RC) heritage represents

✉ Andrea Belleri
andrea.belleri@unibg.it

Extended author information available on the last page of the article

a wide portion of these buildings (Belleri and Marini 2016; Marini et al. 2017; Labò et al. 2017; Belleri et al. 2016; Feroldi et al. 2013). Therefore, their seismic vulnerability presents a huge risk in terms of human safety and economic losses. Conceived as part of the lateral force resisting system for new buildings, pin-supported (PS) walls (also referred to as rocking walls, rocking cores, spine systems or hinged walls) may also represent a possible retrofit solution aimed at linearizing the deformation of the frame along its height (Belleri et al. 2016; Wada et al. 2011; Wada 2018; MacRae et al. 2004) and thus at reducing the inter-storey drift concentration. In the case of existing buildings, a PS wall system can be obtained by connecting new walls from outside, or by re-engineering some of the existing structural elements to this function, such as the stairwell walls (Belleri et al. 2016) (Fig. 1). The main characteristic of the PS walls is the explicit pinned constraint at the base, which transfers only vertical and horizontal loads to the new foundation system (including the wall self-weight and any interaction forces between the wall and the frame). The pin-supported walls can be either simply connected at the storey level through "truss connections" (Fig. 1), by forcing the compatibility of deformation between the frame and the wall, or coupled with the frame by introducing additional replaceable devices (Wada et al. 2009) connected to the existing buildings at the floor levels and/or at the foundation level. In this case, such devices may be designed to provide enough stiffness to reduce damage for low-intensity earthquakes, i.e. possibly working in the elastic range, and to dissipate energy for high-intensity earthquakes. By introducing a PS wall, a change of the static scheme in the original frame is expected; indeed, either due to the change of the deformed shape or for the further bending moment and shear actions introduced at the connection to the existing building, a change of the internal actions along the existing elements occurs. In the case of devices connecting the PS wall to its foundation, the latter would require the transfer of additional shear loads and bending moments, i.e. the pinned constraint becomes a rotational spring.

In the last decade, the application of PS walls from outside as retrofit solution has increased in different countries (Wada et al. 2011; Gioiella et al. 2017). To the authors' knowledge, one of the first applications was reported by Wada et al. (2011): PS walls with steel dampers were implemented in the seismic retrofit of an 11-storey RC frame in Japan. The system is characterized by: the presence of the explicit pinned constraint at the base of the wall, the use of steel dissipation devices along the height of the wall in correspondence of the connection with the existing frame to increase energy dissipation capacity through sacrificial elements replaceable after the earthquake, and the application of post-tension within the wall to increase the wall flexural strength. The design criteria were chosen to

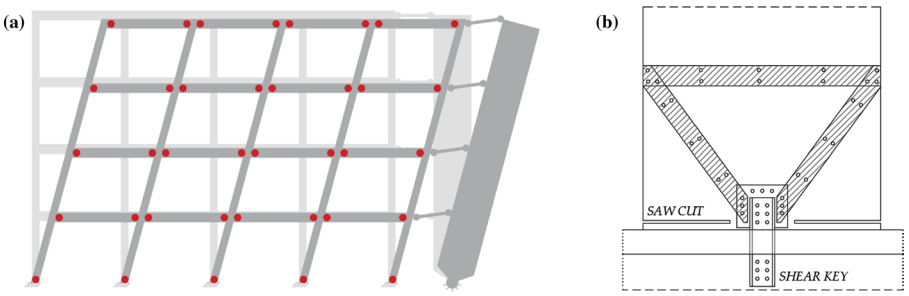

Fig. 1 Example of pin-supported wall solution (**a**) and redesign of a stairwell wall base section (**b**). Adapted from Belleri et al. (2016)

maintain the wall elastic and the inter-storey drift ratio below 1/200 under a major seismic event. The dissipating devices are activated by the vertical relative displacement in correspondence of the wall-frame connection, due to global lateral deformation. In another application, Qu et al. (2012) highlight the load distribution in the retrofitted system and investigate its efficiency through a numerical simulation: the increase of internal actions in some elements of the frame is relevant, for example, in the columns connected to the dampers, which have to transfer larger axial loads. The retrofitted system implemented in Japan also experienced a real earthquake in 2011. Such event allowed to evaluate its behaviour in terms of performance and registered damage, as detailed in Qu et al. (2015a). It was observed that the PS walls major effect on the system behaviour was to make the seismic response less sensitive to design uncertainties, such as the earthquake characteristics and the role of non-structural elements, for example internal partitions. During the earthquake, the PS walls worked in the elastic range as designed, no damage was observed on them, while yielding was detected in some steel dissipators. In Italy, a similar retrofit system was recently implemented in two school buildings (Gioiella et al. 2017; Balducci and Castellano 2015), where external steel truss towers were rigidly connected to the existing structure at the floor levels; in both cases, viscous dampers were placed vertically at the base corners of the towers to dissipate energy by exploiting the towers lateral deformation in the case of earthquakes. Qu et al. (2015b) carried out finite element simulations to investigate the effectiveness of the PS wall retrofit technology: seismic retrofit interventions were simulated by adding RC walls to existing deficient concentrically braced frames, either with or without an energy dissipation connection system. The most efficient range of stiffness ratio between the new PS wall and the structure, in order to reduce the maximum inter-storey drift, was found to lie in the range 0.01–0.3; beyond such value, the effect of the retrofit becomes less remarkable. Bozdogan and Öztürk (2016) proposed an analytical method for the dynamic analysis of the frame-pin-supported wall system, providing dynamic characteristics such as fundamental period, maximum top displacement, and maximum drift for the first three modes of vibration. MacRae et al. (2004) introduced a closed-form solution to relate drift concentration factor, wall stiffness, and strength for a 2D 2-storey concentrically braced frame with uniform strength over the height and empirical formulations to account for multi-storey buildings with variable strength over the height. Equations were developed to estimate the drift concentration factor (ratio between the maximum and minimum inter-storey drift ratios) and the column moment demand for a frame subjected to pushover analysis. Blebo and Roke (2015) introduced preliminary design criteria for self-centring rocking core systems applied to conventional braced frames: in this case, the RC core presents vertically oriented post-tensioning bars that provide additional overturning moment capacity and prevent RC core from cracking and the resulting wall stiffness degradation. Pan et al. (2015) proposed a closed-form distributed-parameter model to investigate the behaviour of the retrofitted system subjected to three typical lateral load patterns by using a continuum method of analysis: the displacement of the system, along with the shear and moment demands both for the frame and the wall for a uniform or inverted triangular load pattern or for a concentrated force at the top can be computed in the elastic field by solving differential equations. The same continuum analysis approach was followed by Rahgozar et al. (2018), who investigated the effect of the wall base rotational stiffness and the relative stiffness between the wall and the frame. Recently, Zhou et al. (2021) developed an upgraded parameter model, where a lumped mass model simulates the frame behaviour under seismic loading, the wall and the frame are connected only at storey levels, and a variation of the frame stiffness along the height is considered. Finally, Sun et al. (2017) extended the distributed parameter model developed by Pan et al. (2015)

to include also dampers placed at the wall-frame connections along the vertical direction, focusing on the effects of the damper stiffness on the wall-frame interaction. Furthermore, they proposed a performance-based plastic design approach for pin-supported wall-frame structures which was validated through numerical simulations.

Most of the previous researchers assumed a constant storey lateral stiffness of the frame along its height in developing analytical models to describe the frame-pin-supported wall retrofitted system; previous results presented by the authors (Casprini et al. 2019) show that such simplified assumption may not be conservative when dealing with PS wall implemented as retrofitting of existing structures. The weaknesses and the possible beneficial effects of PS walls applied to some typical configurations of RC existing frames were investigated: the beam to column capacity ratio was found to be a key parameter for identifying the best configuration of the retrofit solution. Some computational aspects were also investigated to obtain a reliable estimate of the actual behaviour of the existing structure, such as the actual moment-axial forces interaction for the columns and the actual distribution of gravity loads on the beams. Since in some cases the high deformation demand due to the introduction of the PS wall can be critical for the structural elements, a possible solution was proposed by modifying the number and configuration of links along the building height (Casprini et al. 2019).

The present paper provides a procedure to preliminarily assess the suitability of the PS wall solution as a seismic retrofit system for existing RC frames. The retrofitted system modelled herein is composed of an existing 2D frame and an additional PS wall, thus only planar effects are considered; regular frames are examined, with no reduction of the column cross-section along the height, nor irregular distribution of infills. A shear type behaviour is preliminarily assumed for the existing RC frame to derive a closed-form solution for the PS wall design and because such hypothesis may be particularly suitable for RC frames designed before the enforcement of modern anti-seismic regulations, therefore not compliant with the strong column-weak beam approach. Corrective factors are also provided to account for non-shear type conditions. The proposed simplified analytical method aims at investigating the potential benefits derived from the application of PS walls in terms of a capacity increase of the retrofitted system and at providing the internal actions in the PS wall to allow for a preliminary design. The increase of the global seismic capacity is also assessed considering the application of additional devices, placed between the wall and the existing RC frame or connecting the wall base and its foundation.

The proposed set of equations accounts specifically for the first fundamental mode of vibration of the retrofitted system. It is expected that the higher modes of vibrations would predominantly act as additional loads on the PS wall which would lead to an increase of the bending moment demand along the wall height. Such increase is related to the modal parameters of the retrofitted system and to the seismic input. The additional flexural demand would require an increase of the amount of reinforcing bars in the PS wall and possibly to the increase of the cross-section dimensions. However, it is worth mentioning that such changes would not compromise the evaluation of the beneficial or detrimental effects of PS wall retrofit solutions addressed in this paper and the estimate of the wall demand according to the first mode of vibration. The effect of higher modes of vibrations may be considered for instance by applying the methods reported in Sullivan et al. (2008), Wiebe and Christopoulos (2015), and Rahgozar and Rahgozar (2020) among others and it is a topic of ongoing research.

Once the beneficial effects derived from a PS wall retrofit solution have been assessed in terms of load capacity increase and the preliminary size of the PS wall has been defined, the assessment of the required ductility demand in the existing elements must be carried

out to evaluate the effectiveness of the proposed solution or to highlight existing elements requiring local retrofit interventions to enhance their ductility capacity. This assessment can be carried out for instance by means of a pushover analysis of the retrofitted system. In the future, this aspect may be treated analytically and implemented in the model. The validation of the proposed set of equations has been carried out by means of non-linear finite element analyses.

2 Pin-supported walls as a retrofit system

The principal aim of implementing a pin-supported wall in the retrofit of existing structures is to linearize the lateral deformation of the building along its height, thus correcting possible in-elevation irregularities and avoiding excessive deformation demand concentration in single storeys, which may lead to soft storey mechanisms. For this purpose, the minimum wall stiffness required to exploit such a function needs to be defined by considering the lateral stiffness ratio between the PS wall and the frame, i.e., the parameter χ in Eq. (1). Such parameter was adapted from MacRae et al. (2004), who provided a formulation for 2-storey frames. In Eq. (1), the lateral stiffness ratio is calculated, in which the total height of the building H_T is substituted to the inter-storey height (MacRae et al. 2004) for a wider extension of the applicability to multi-storey frames:

$$\chi = \frac{E_w I_w}{K_s H_T^3} \tag{1}$$

where K_s is the frame storey lateral stiffness of the generic intermediate storey (if relevant differences between storeys are present, a mean value may be preliminarily assumed); E_w and I_w are the elastic modulus and the moment of inertia of the PS wall, respectively. Sensitivity analyses were carried out through elastic finite element models of 2D frames varying between 3 and 8-storey in order to identify the value of χ required to linearize the frame deformation in the elastic range; the characteristics of an intermediate storey of a regular frame were considered to calculate the mean storey lateral stiffness (5-bays frame B described in Sect. 3.1, with $K_s = 26{,}555$ kN/m). The same formulation applies in elastic models where stiffness is reduced to account for cracking of the existing RC elements.

Herein, the dimensions of the PS wall were defined by setting the value of χ and calculating the wall moment of inertia I_w through Eq. (1). The linearization effect of the PS wall was evaluated through the drift concentration factor (DCF), computed as the ratio between the maximum and the minimum inter-storey drift along the height of the frame. A complete linearization occurs in correspondence of DCF equal to 1. It was found (Fig. 2) that for $\chi > 0.05$ the corresponding DCF was always lower than 1.2. Furthermore, beyond $\chi = 0.5$ the deformation is linearized and there is no further beneficial effect deriving from the increase of the wall dimensions. Therefore, in the following applications, values of χ equal to 0.5 are assumed (DCF always lower than 1.02); it is worth noting that, for engineering purposes, less demanding stiffness ratio, such as χ equal to 0.3 (DCF lower than 1.05), could be considered. For different frame typologies, as for instance in the case of soft storeys or columns with reduced cross-section along the building height, the value of χ which is effective in linearizing the frame deformation should be reconsidered; however, relevant differences were not observed by varying the number of bays or reducing the columns cross-section of 10% at each storey level along the building height. In all the examined cases, it was observed that for $\chi \geq 0.1$, the DCF tends to 1.

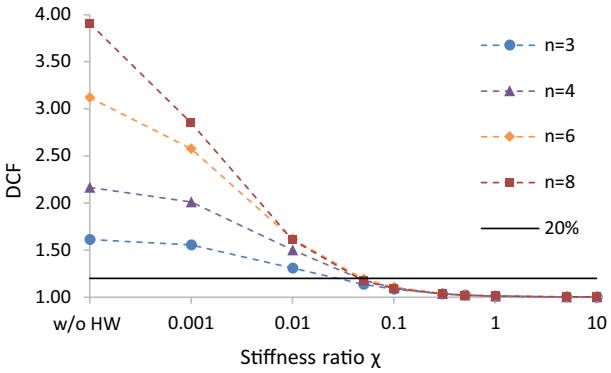

Fig. 2 Drift concentration factor (DCF) distribution for n-storey frame, having constant frame storey lateral stiffness (K_s) along the height, by varying the PS wall flexural stiffness for selected values of χ

Concerning the frame storey lateral stiffness ($K_{s,j}$), the formula proposed by Schultz (1992) was adopted (Eq. 2). The expression considers regular frames, fixed at the base, and accounts only for flexural deformations:

$$K_{s,j} = \left(\frac{24}{H^2}\right)\left(\frac{1 + C_{s,j}}{\frac{2}{\sum k_c} + \frac{1}{\eta_a \sum k_{ga}} + \frac{1}{\eta_b \sum k_{gb}}}\right) \tag{2}$$

where H is the inter-storey height; $\sum k_c$ is the sum of the stiffness of the columns in a given storey; $\sum k_{ga}$ and $\sum k_{gb}$ are the sum of the flexural stiffness of the girders framing into the joint above and below the columns, respectively. The stiffness of each member (column or girder) is calculated as $k = EI/L$. The coefficients η_a and η_b account for possible different inter-storey heights and they are assumed equal to 1 in regular frames. $C_{s,j}$ (j is the storey of interest) is a corrective factor which accounts for different boundary conditions at each storey, particularly for the first storey ($C_{s,1}$ in Eq. 3), whose columns are fixed to the ground. For any intermediate storey, $C_{s,j}$ is herein assumed equal to zero. Given the frame geometry and the structural element dimensions, the PS wall moment of inertia I_w is obtained from Eq. (1); then, the length of the wall cross-section L_w is calculated as in Eq. (4), where t_w is the cross-section depth.

$$C_{s,1} = \frac{\sum k_c}{22 \sum k_{ga}} \tag{3}$$

$$L_w = \sqrt[3]{\frac{12 I_w}{t_w}} \tag{4}$$

A scheme of the behaviour of the retrofitted system is shown in Fig. 3. The introduction of the PS wall allows transferring a portion of the seismic horizontal loads from the frame to the wall. The strength of the existing structural elements at a sectional level does not change, but the new configuration allows a different internal distribution of the loads which may provide an increase of the global seismic capacity. It is worth noting that due to the deflected shape linearization the loads transferred between the wall and the frame can be either compression or tensile actions, as it will be presented in the next session.

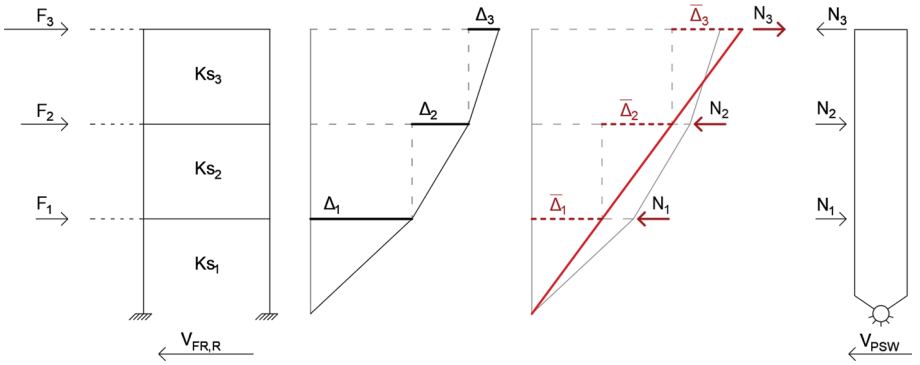

Fig. 3 Example of the linearization of the frame deformation along its height for a 3-storey frame. Note: only one bay of the frame is represented for sake of clarity

In the case of rigid truss elements connecting the frame and the wall at the storey levels, the horizontal displacement compatibility is enforced between the two systems, leading to a change in the static scheme; the deflected shape is governed by the flexural stiffness of the wall through the coefficient χ; the links act as rigid spacers and transfer only axial loads. The global stiffness of the coupled system, as it results from the enforced linearized deformation, depends on the characteristics and configuration of the existing frame. In the case of regular frames, a negligible stiffness increase is observed, while for other configurations, such as in the case of columns with decreasing cross-section along the building height, a significant stiffness increase may be observed. Moreover, various connecting elements may be introduced, either in substitution of the aforementioned truss elements or as additional dissipating systems; the introduction of such elements leads to a further constraint of the existing building structural elements, thus to a further redistribution of the internal actions in the existing frame and in the new wall. As schematically represented in Fig. 4, these devices may be placed either between the wall and the existing frame at the floor levels (transferring also shear and bending moment) and/or between the wall and its foundation (transforming the pinned constraint into a non-linear rotational spring); in the former case, the capacity of the frame structural elements in transferring the coupling forces should be checked, while in the latter, the foundation system needs to provide adequate flexural capacity. The additional contribution provided by such devices is included in the following analytical method by accounting for the associated equivalent resisting bending moment $\overline{M}$, which entails an increase of the pin-supported wall base shear, herein referred to as ΔV_d. $\overline{M}$ is related to the activation loads in the additional devices as in Eqs. (5), (6), (7), for devices at the wall base ($\overline{M}_A$ from Fig. 4a), distributed devices at floor levels on one side of the wall ($\overline{M}_B$ from Fig. 4b) or on both sides of the wall ($\overline{M}_C$ from Fig. 4c), respectively. Regardless of the device's configuration, the expression obtained for ΔV_d is reported in Eq. (19) for the elastic range and in Eq. (27) for the plastic range.

$$\overline{M_A} = F_d \cdot L_w \tag{5}$$

$$\overline{M_B} = \sum_{i=1}^{n} \left(f_{d,i} \cdot \frac{L_w}{2} + m_{d,i} \right) \tag{6}$$

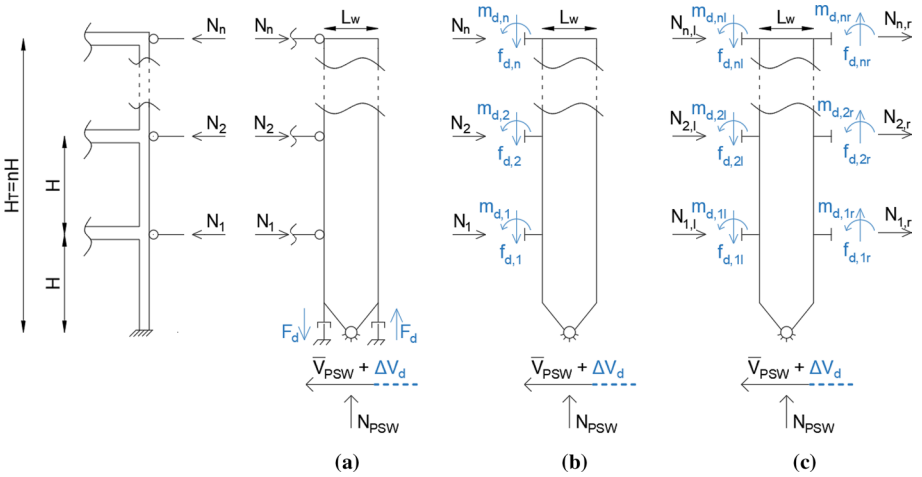

Fig. 4 Pin-supported wall with an example of coupling with three different systems of additional devices: internal actions providing the additional contribution to the base shear (ΔV_d) are represented in blue; "l"-left, "r"-right

$$\overline{M_C} = \sum_{i=1}^{n} \left(f_{d,il} \cdot \frac{L_w}{2} + f_{d,ir} \cdot \frac{L_w}{2} + m_{d,il} + m_{d,ir} \right) \tag{7}$$

3 Elastic load distribution in the pin-supported wall and in the existing frame

Considering that the PS wall retrofit solution modifies the distribution of loads and internal actions in the system, an analytical method for the calculation of the shear demand at the frame base $V_{FR,R}$ and at the wall base V_{PSW} is herein proposed. The retrofitted system behaviour can be analytically investigated in the elastic range by assuming a shear type behaviour, therefore the beam deformability is neglected, and a rigid translation of each storey is assumed. Corrective factors are provided in the following to account for the actual beam flexibility. The elastic distribution of loads and internal actions in the frame and in the wall before and after the PS wall application has been investigated through equilibrium equations and deformation compatibility. Herein, a closed-form solution is obtained for n-storey frames with constant inter-storey height H and with a constant lateral storey stiffness ($K_{s,j}=K_s$ for $j=2{:}n$) for all the storey but the 1st one, in which the stiffness is assumed equal to $K_{s,1}=\beta K_s$. In Sect. 3.1, this assumption is discussed and some typical values of β are investigated. The seismic action is represented as point loads at each floor level (F_i in Fig. 5), with an inverse triangular pattern due to the linearization of the deformed shape provided by the PS wall, according to the 1st vibration mode; at the ith storey, F_i is expressed as in Eq. (8), where i is the floor number, H (m) is the storey height and α (N/m) is a coefficient relating the external seismic load (assumed as linearly distributed) with the storey level. As stated before, higher mode effects are not directly addressed in this

preliminary evaluation, although their influence could be estimated with available methods (e.g. Sullivan et al. 2008; Wiebe and Christopoulos 2015; Rahgozar and Rahgozar 2020). It is worth mentioning that a possible increase of the PS wall cross-section to accommodate the additional bending moment deriving from higher modes of vibration would not compromise the analytical formulations and the considerations addressed in the paper.

The storey shear at each level V_j is obtained from the sum of the loads F_i and N_i of the storeys above it (Eq. 9), where N_i is the load transferred between the frame and the wall at the ith level. Before the PS wall introduction, the equations are still valid with $N_i = 0$ under the assumption of a linear load distribution.

$$F_i = i\alpha H \tag{8}$$

$$V_j = \sum_{i=j}^{n} (i\alpha H + N_i) = 0 \tag{9}$$

In the elastic field, the storey lateral displacement is computed as the ratio between the storey shear V_j and the storey lateral stiffness $K_{s,j}$, both in the as-is condition (Eq. 10) and after the PS wall introduction (Eq. 11). The equations governing the problem are identified as: (i) the condition of equal inter-storey displacements between adjacent storeys due to the deformed shape linearization in the frame; (ii) the moment equilibrium with respect to the pinned connection at the wall base (Eq. 12). By imposing an equal inter-storey drift between two generic consecutive floors j and $j+1$, with j varying from 2 and n−1, the value of N_j is derived (Eq. 13). Therefore, if the storey lateral stiffness is constant along the height of the frame, the load transferred from the frame to the wall at each floor level is equal to the seismic action applied at the same level, for the 2nd to the (n−1)th floor level; the loads transferred to the PS wall at the 1st (N_1) and top floor level (N_n) are calculated from the system of two Eqs. (14), leading to Eqs. (15) and (16), respectively. The detail of the solution is reported in Appendix 1.

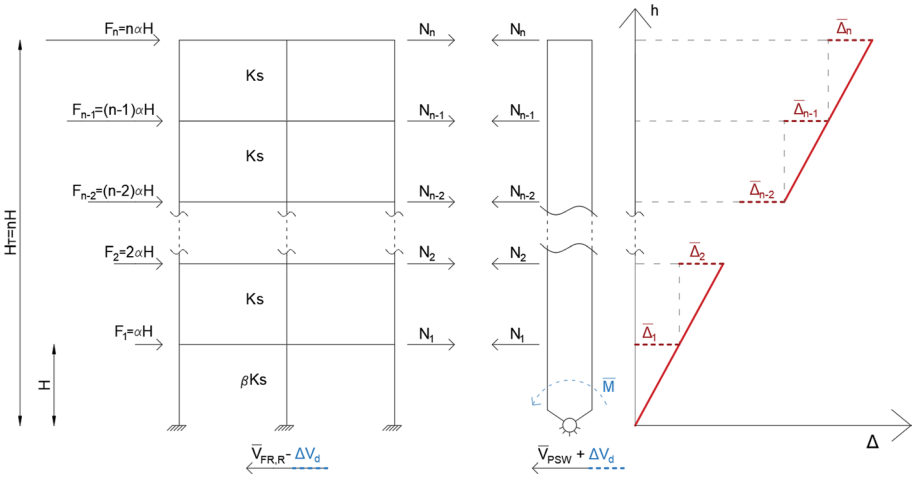

Fig. 5 Forces distribution after PS wall introduction. $\overline{M}$ represents the equivalent additional resisting moment in the case of additional devices, as described in Fig. 4 and Eqs. (5)–(7)

$$\Delta_j = V_j / K_{s,j} \tag{10}$$

$$\overline{\Delta_j} = \frac{\sum_{i=j}^{n} (i\alpha H + N_i)}{K_{s,j}} \tag{11}$$

$$\begin{cases} \overline{\Delta_{j+1}} = \overline{\Delta_j} \ \text{for} \, j = 1 : n-1 \\ \sum M_0 = 0 \end{cases} \tag{12}$$

$$N_j = -j\alpha H \ \text{ for} \, j = 2 : n-1 \tag{13}$$

$$\begin{cases} \overline{\Delta_2} = \overline{\Delta_1} \\ \sum M_0 = 0 \end{cases} \rightarrow \begin{cases} \frac{\sum_{i=2}^{n} i\alpha H + N_i}{K_s} = \frac{\sum_{i=1}^{n} i\alpha H + N_i}{\beta K_s} \\ N_1 H - \alpha H^2 \sum_{i=2}^{n-1} i^2 + N_n n H + \overline{M} = 0 \end{cases} \tag{14}$$

$$N_1 = \frac{\alpha H}{6} \frac{(2n^3 + 3n^2 - 6)(\beta - 1) + n(\beta - 7) + \frac{6\overline{M}}{\alpha H^2}(1 - \beta)}{n + \beta - 1} \tag{15}$$

$$N_n = \frac{\alpha H}{6} \frac{(2n^3 - 3n^2 + 7n - 6\beta n) - \frac{6\overline{M}}{\alpha H^2}}{n + \beta - 1} \tag{16}$$

Since the internal force distribution is known, the PS wall base shear (V_{PSW} in Eq. 17) is computed as the sum of all N_i; the frame base shear after the PS wall introduction ($V_{FR,R}$ in Eq. 18) is obtained from the difference between the total seismic load and the PS wall base shear. For the sake of completeness, the aforementioned equations contain the contribution of the additional devices reported in the previous section (Fig. 4) in terms of ΔV_d. Such contribution is represented by the terms including $\overline{M}$.

$$V_{PSW} = \overline{V}_{PSW} + \Delta V_d = \frac{\alpha H}{6} \frac{(n^3 - n)(3 - 2\beta)}{n + \beta - 1} + \Delta V_d \tag{17}$$

$$V_{FR,R} = \overline{V}_{FR,R} - \Delta V_d = \frac{\alpha H}{6} \frac{n\beta(2n^2 + 3n + 1)}{n + \beta - 1} - \Delta V_d \tag{18}$$

$$\Delta V_d = \frac{\beta}{H} \frac{\overline{M}}{n + \beta - 1} \tag{19}$$

3.1 Considerations on the lateral stiffness of the frame

The proposed formulation includes a coefficient β which accounts for the possible difference of storey lateral stiffness at the 1st storey, which may be different than the others

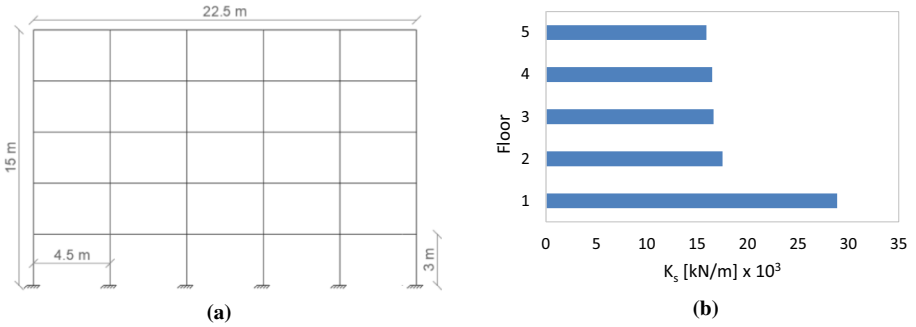

Fig. 6 Frames geometry (**a**) and example of storey lateral stiffness evaluation (**b**) for frame A. Adapted from Casprini et al. (2019)

due to the different boundary conditions, interstorey height, lack of infills, etc. In regular frames, where neither reduction of the column cross-section along the height nor irregular distribution of the infilled walls characterize the structural layout, modest differences between the lateral stiffness of consecutive intermediate storeys are considered negligible in terms of the global behaviour of the retrofitted system, while the 1st storey lateral stiffness may be more relevant.

A simple estimation of the storey lateral stiffness has been carried out to define possible values of β, referring to the four frames (Fig. 6 and Table 1) described in Casprini et al. (2019), which account for some typical features of existing regular RC structures. Case A and Case B represent a frame with weak beams and strong columns and a frame with strong beams with respect to columns, respectively; in case C and D, these characteristics are further emphasized with respect to A and B. In all frames, the columns dimension is 30 cm × 30 cm, with a concrete cover c = 3 cm and 4 ϕ16 as reinforcement (except for case C, with 4 ϕ20); as for the beams, their geometry and detailing are different for each frame to obtain different beam to column capacity ratios. Beams structural details are reported in Table 1; a concrete modulus of elasticity equal to $E_c = 31476$ MPa [C25/30 according to EN 1992 (2004a)] is adopted; flexural stiffness of beams and columns is reduced to 50% and 70%, respectively, to account for concrete cracking.

The assessment was carried out through both numerical simulations and analytical computations. As for the former, a horizontal force was applied in turn at each floor level and the inter-storey displacement between the storey of interest and the one below was computed through the software MidasGEN (2020); the lateral stiffness was calculated directly as the ratio between the applied force and the measured displacement. The storey lateral stiffness was also analytically computed (Table 2) by applying Eq. (2) (Schultz 1992) and

Table 1 Beam cross-section detailing. Note: b and h are the cross-section dimensions, c is the concrete cover thickness, A_{sb} and A_{st} are the longitudinal rebars at the bottom and top, respectively

Beam details				Beam ends		Beam centre	
Case	b (cm)	h (cm)	c (cm)	A_{sb}	A_{st}	A_{sb}	A_{st}
A	80	24	3	3ϕ16	9ϕ16	6ϕ16	3ϕ16
B	30	35	3	3ϕ16	4ϕ16	3ϕ16	3ϕ16
C	80	24	3	3ϕ16	6ϕ16	4ϕ16	3ϕ16
D	30	50	3	3ϕ16	4ϕ16	3ϕ16	3ϕ16

assuming the corrective factor $C_{s,j}$ equal to zero for intermediate storeys and by calculating its actual value for the 1st storey, as in Eq. (3). In all cases, it was found that the lateral stiffness of the 1st storey is higher than the others, and that β is in the range $1 \div 2$ for the considered frames. It is worth noting that a higher and a lower value of β is obtained in the case of a lower and a higher 1st storey height, respectively.

3.2 Application of the pin-supported wall to a 3-storey frame

In order to show the effectiveness of the provided method in estimating the behaviour of the retrofitted system, the formulation is applied to a 3-storey frame retrofitted with a PS wall without additional devices; the linearization of the deformed shape of the frame subjected to horizontal loads is inherently assumed in the proposed analytical model, thus the lateral stiffness ratio (χ) between the PS wall and the frame has to be set at least equal to 0.3–0.5. The elastic forces distribution before and after the retrofit has been calculated by adopting three different values of the coefficient β: $\beta = 1$ is assumed to represent the hypothesis of constant storey lateral stiffness along the height; $\beta = 2$ is an upper bound considered to represent a higher stiffness of the 1st storey (from Table 2); $\beta = 0.7$ is taken into account (Fig. 7) to consider the case of a smaller 1st storey lateral stiffness (for example in case of a higher 1st storey or a pilotis structure).

It is observed that the value of β alters the shear distribution in the frame; accordingly, an amplification factor can be derived by evaluating the seismic action, following a triangular distribution, which provides the same base shear in the frame without ($V_{FR,0} = \alpha Hn(n+1)/2$) and with ($V_{FR,R}$ from Eq. 18) the PS wall. Such factor is thus defined as $V_{FR,0}/V_{FR,R}$. Therefore, an amplification factor greater than 1 means that the retrofit intervention is potentially beneficial, otherwise the retrofit may have a detrimental effect in terms of global capacity. It is observed that when $\beta = 1$, $V_{FR,0}/V_{FR,R} = 1.29$, but when $\beta > 1$ the ratio may be smaller than 1 ($V_{FR,0}/V_{FR,R} = 0.85$ for $\beta = 2$). A significant beneficial effect is observed instead for $\beta = 0.7$, with $V_{FR,0}/V_{FR,R} = 1.65$. Considering Fig. 7, it is clear that the system behaviour is governed by the compatibility of deformation between the frame and the wall: for all the considered values of β, at the top floor the storey shear in the frame is increased after the PS wall introduction, whereas at the first level the behaviour is a function of β: for $\beta \leq 1$, the PS wall leads to a reduction of the storey shear in the frame.

Table 2 Storey lateral stiffness estimation

	Method	1st storey $K_{s,1}$ (kN/m)	$C_{s,1}$	Generic storey K_s (kN/m)	β
CASE A	Numerical	28,902		16,644*	1.74
	Eq. (2)	22,356	0.084	13,937	1.60
CASE B	Numerical	30,148		18,069*	1.67
	Eq. (2)	23,709	0.072	15,331	1.55
CASE C	Numerical	28,835		16,650*	1.73
	Eq. (2)	22,356	0.084	13,937	1.60
CASE D	Numerical	34,916		27,153*	1.29
	Eq. (2)	31,945	0.025	25,680	1.24

*Represents the mean value of the lateral stiffness of the storeys above the 1st one

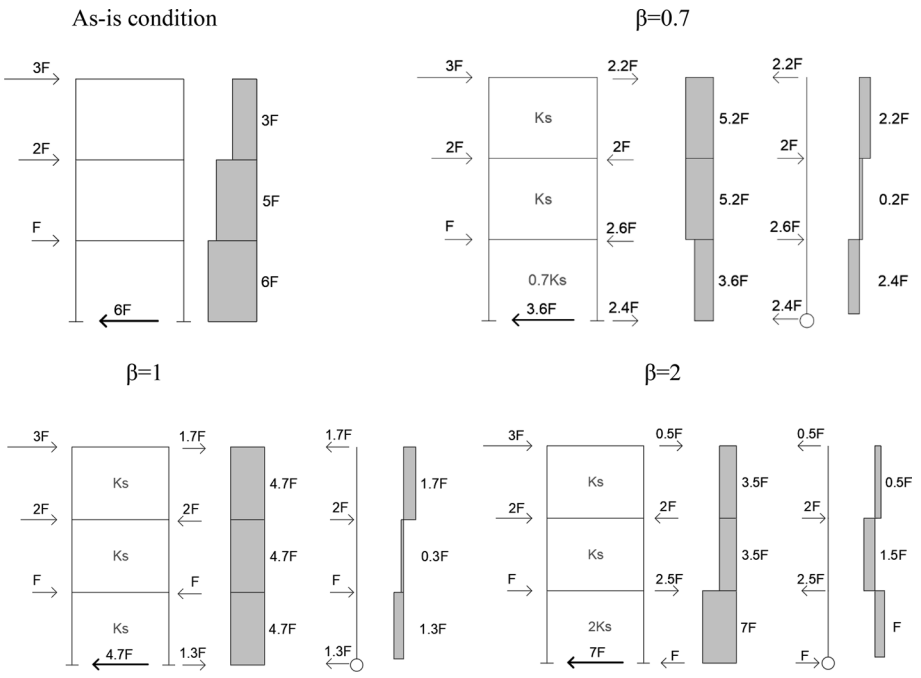

Fig. 7 Shear distribution in the frame for a total seismic load equal to 6F ($\alpha = F/H$), forces transferred to the PS wall and shear distribution in the PS wall for a 3-storey frame for different values of β. Note: only one bay of the frame is represented in the figure for sake of clarity

Conversely, for a larger stiffness of the first storey ($\beta = 2$), the deformed shape linearization leads to a further increase in the storey shear at the first level. Because the application of the PS wall may be detrimental under some conditions, new solutions have been investigated (Casprini et al. 2019) by changing the number and the configuration of connecting links between the existing frame and the wall. For sake of clarity, the same concept is represented graphically in Fig. 8 in terms of frame and PS wall base shear in the as-is condition (FR), after the PS wall introduction (FR + PSW), and after placing additional devices (FR + PSW + $\overline{\text{M}}$).

The analyses were carried out by considering the same triangular distribution of the seismic loading for all the cases, which leads to the same total seismic action referred to as 100%; these assumptions do not influence the results considering that elastic analyses are carried out. For $\beta = 0.7$ and $\beta = 1$, the adoption of a PS wall leads to a smaller share of shear action undertaken by the existing frame, while the opposite happens for $\beta = 2$, where an increase of the frame base shear is observed and a consequent base shear in the opposite direction arises in the PS wall. For this reason, a possible floor stiffness variation over the height must be carefully taken into account when designing a PS wall retrofit system. The further introduction of additional devices mitigates such effect. These results are associated with an elastic behaviour of the frame and of the wall. The contribution of inelasticity will be addressed in a following section. Figure 9 shows the amplification factor ($V_{FR,0}/V_{FR,R}$, Sect. 3.2) for a n-storey frame, with n varying from 2 to 10, by applying the proposed equations. According to the proposed formulation, the amplification factor depends on the

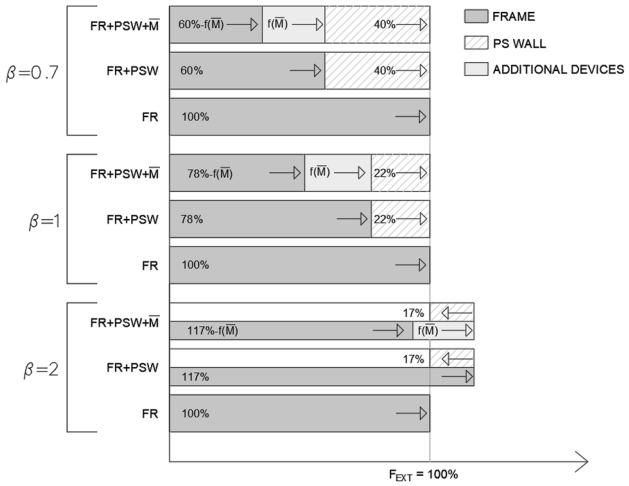

Fig. 8 Share of base shear with respect to the total external load (100%) applied for a 3-storey frame ($\beta=0.7$, $\beta=1$ and $\beta=2$) in the as-is configuration (FR), after the PS wall introduction (FR + PSW) and with additional devices (FR + PSW + $\overline{M}$)

stiffness ratio β, and not on the geometrical properties of the structural elements; thus, the trend presented in Fig. 9 holds for frames with different number of storeys, even if different element dimensions would be expected by increasing n.

For the sake of simplicity, the contribution of additional devices is neglected ($\overline{M}=0$). It can be noticed that for $\beta=2$, i.e. stiffness of the 1st storey doubled with respect to the other storeys, the factor $V_{FR,0}/V_{FR,R}$ is always smaller than 1 and the PS wall may be detrimental unless further engineering of the solution is developed; on-going research on the topic is being carried out by the authors. Figure 9 highlights an asymptotic trend of $V_{FR,0}/V_{FR,R}$ (to 3/2β) when the storey number increases: for $\beta=0.7$ the maximum value is 2.14, for $\beta=1$ the maximum value is 1.50, while for $\beta=2$ the minimum amplification factor is 0.75. It is worth noting that this complies with the results presented in MacRae et al. (2004), who obtained a maximum increase of the shear capacity of a 2-storey frame equal to 1.2 after the introduction of stiff continuous columns, which could be seen as equivalent to a PS wall introduction. It can also be analytically proved that the amplification factor is always smaller than 1 for $\beta \geq 1.5$, which can be considered as the threshold value corresponding to a possible detrimental behaviour of the retrofitted system.

3.3 Sensitivity analysis for non-shear type conditions

The previous analytical formulation was derived assuming a shear type behaviour of the existing frame: a rigid translation of each storey was considered, and the axial and flexural deformability of beams was neglected. This assumption has the advantage to provide a straightforward analytical model suitable for a preliminary assessment of the benefits of a PS wall solution, its demand in terms of internal actions and in the case of strong-beams and weak-columns frames. To adapt the proposed model to conditions different from the shear-type assumption, a sensitivity analysis was conducted, and a corrective factor was defined for the calculated maximum bending moment in the PS wall. Such a corrective

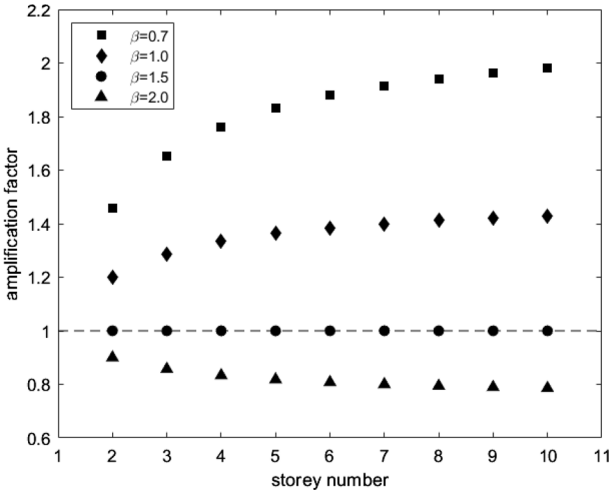

Fig. 9 Amplification factor $V_{FR,0}/V_{FR,R}$ for frames up to 10 storeys ($\chi \geq 0.5$) for different values of β

factor is the ratio between the maximum bending moment along the PS wall height in the elastic phase obtained from a finite element analysis and from the proposed analytical formulation, considering that the bending moment is the main internal action adopted in the preliminary design of this retrofit system. Various parameters were considered such as the number of storeys (n = 3, 5, 8), the storey lateral stiffness ratio ($\beta = 0.7$, $\beta = 1$, $\beta = 2$), and a further parameter accounting for the difference between the real behaviour and the assumed shear type behaviour ($K_s/K_{S.T}$), defined as the ratio between the generic storey lateral stiffness K_s (Eq. 2 for the intermediate storey, that means with $C_s = 0$) and the storey lateral stiffness in the case of shear type behaviour $K_{S.T}$ (Eq. 2 as above with infinite stiffness of the girders above and below the floor, i.e. k_{ga}, $k_{gb} \rightarrow \infty$). By assuming a linear distribution of the external load, the ratio between the PS wall bending moment obtained from a finite element simulation and the proposed analytical formulation was calculated. The results of the sensitivity analysis are reported in Table 3; a linear interpolation is suggested in between depending on the effective geometrical characteristics of the existing frame.

It can be noted that the difference from the actual maximum bending moment increases by getting further from the ideal shear type frame behaviour (low $K_s/K_{S.T}$ values), when the storey number decreases and when β increases. In fact, all these factors contribute to making the characteristics of the frame less homogeneous along the height, entailing secondary effects which are not included in the analytical model, as for example differences in the storey lateral stiffness (beyond the 1st one) or the influence of the beam flexibility.

4 Capacity of the retrofitted system

The elastic load distribution of the structure before and after the retrofit intervention is useful to perform preliminary evaluations of the possible benefits of a PS wall. For design purposes, the capacity of the retrofitted system needs to be investigated considering the capacity of the existing frame, while the PS wall should be designed to be elastic for the target seismic event in order to limit or avoid PS wall repair interventions. An analytical formulation is proposed herein by approaching the problem as previously carried out in the elastic

Table 3 Corrective factor for maximum bending moment prediction in the PS wall ($\chi = 0.5$); according to the convention in Fig. 5, the maximum bending moment is always negative and located in correspondence with the intermediate upper storeys

$K_s/K_{S.T}$	$\beta = 0.7$			$\beta = 1$			$\beta = 2$		
	$n = 3$	$n = 5$	$n = 8$	$n = 3$	$n = 5$	$n = 8$	$n = 3$	$n = 5$	$n = 8$
1	1	1	1	1	1	1	1	1	1
0.8	1.04	1.03	1.02	1.13	1.05	1.03	1.44–1.06*	1.12	1.06
0.5	1.12	1.09	1.05	1.35	1.13	1.08	2.1–1.31*	1.36	1.13
0.2	1.28	1.14	1.10	1.59	1.19	1.15	2.42–2.15*	1.69	1.20

For 3-storey frames, the maximum bending moment is positive and located at the first level; the corrective factor is reported for both negative and positive maximum bending moment

range. In this case, the equations governing the problem are: (i) the equilibrium at each floor level (i.e. accounting for the frame shear below and above the considered floor and the load transferred to the PS wall), and (ii) the moment equilibrium with respect to the PS wall base. A shear type behaviour is considered, and the storey shear capacity is associated with the development of plastic hinges at each column ends. This is a simple and effective way for a preliminary estimation, especially for strong beams—weak columns conditions. The ductility capacity of the existing elements would be assessed through a pushover analysis after the evaluation of the effectiveness of the PS wall in terms of strength. It is also assumed that, before the PS wall introduction, the existing frame maximum capacity is achieved upon reaching the maximum shear capacity in one storey, although, in other existing structures different failure mechanisms may arise. In addition, it is worth mentioning that the effectiveness of the intervention should be clearly checked according to the defined design targets and performance objectives. The shear capacity at each frame level is assumed to be known. If the structural elements have the same geometrical and mechanical properties in the structure, the column capacity depends on the moment-axial load interaction, thus, the actual capacity of the columns decreases along the height of the frame according with the axial load applied. This leads to the definition of $n+1$ equations and $n+1$ unknowns, being n the number of storeys. The unknowns are the loads N_i in the links between the frame and the wall, and the increase of the applied external seismic load until the system maximum capacity is reached (herein referred to an increase of δ_F at each floor level considering the linear deflected shape imposed by the pin-supported wall, Fig. 10).

The proposed formulation is strictly related to the one previously derived for the elastic range, which describes the system behaviour up to yielding. The following formulation allows to extend the results until achieving the shear capacity at each storey. The analytical solution is provided for a n-storey frame with constant inter-storey height H. The seismic action is represented as a linear distribution of lumped loads (F_i) at each floor level; at each storey i, F_i is expressed as in Eq. (20) (Fig. 10). The solution is independent of the storey lateral stiffness and it depends only on the number of storeys and their shear capacity, along with the possible additional moment $\overline{M}$ provided by additional devices. Equations (20)–(25) provide the solution under the hypothesis that the capacity of the frame before retrofit is associated with the capacity of the 1st storey. Analogous formulations can be obtained when the capacity of another storey is first met. The PS wall base shear (V_{PSW}) and the frame base shear ($V_{FR,R}$) are defined in Eqs. (24) and (25), respectively. The complete step-by-step solution is reported in Appendix 2.

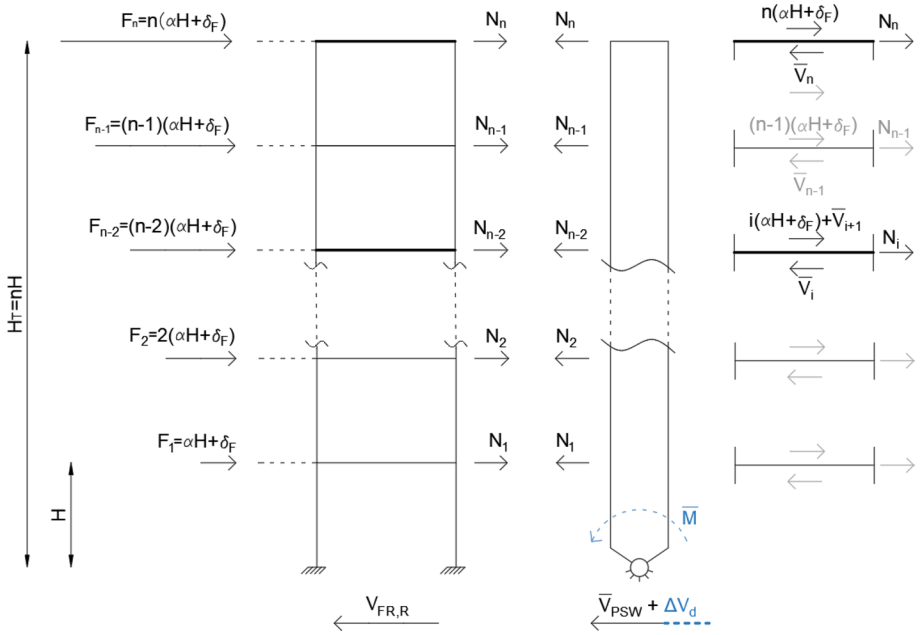

Fig. 10 Capacity of the retrofitted system. Note: only one bay of the frame is represented for sake of clarity. For sake of simplicity, $\overline{M}$ represents the equivalent additional resisting moment in the case of additional devices, as described in Fig. 4 and Eqs. (5)–(7)

$$F_i = (\alpha H + \delta_F)i \tag{20}$$

$$\begin{cases} N_n + n(\alpha H + \delta_F) = \overline{V}_n & \text{for } j = n \\ N_j + j(\alpha H + \delta_F) + \overline{V}_{j+1} = \overline{V}_j & \text{for } j = 1 : n-1 \\ \sum_{i=1}^{n} N_i iH + \overline{M} = 0 \end{cases} \tag{21}$$

$$(\alpha H + \delta_F) = 6\frac{\sum_{i=1}^{n} \bar{V}_i + \frac{\bar{M}}{H}}{n(n+1)(2n+1)} \tag{22}$$

$$\begin{aligned} N_n &= \bar{V}_n - 6\frac{\sum_{i=1}^{n} \bar{V} + \frac{\bar{M}}{H}}{(n+1)(2n+1)} = \bar{V}_n - n\left(\alpha H + \delta_F\right) \\ N_i &= \bar{V}_i - \bar{V}_{i+1} - 6i\frac{\sum_{i=1}^{n} \bar{V} + \frac{\bar{M}}{H}}{n(n+1)(2n+1)} = \bar{V}_i - \bar{V}_{i+1} - i\left(\alpha H + \delta_F\right) \end{aligned} \tag{23}$$

$$V_{PSW} = 3\frac{\sum_{i=1}^{n} \bar{V}_i + \frac{\bar{M}}{H}}{(2n+1)} - \bar{V}_1 = (\alpha H + \delta_F)\frac{n(n+1)}{2} - \bar{V}_1 \tag{24}$$

$$V_{FR,R} = \overline{V}_1 \tag{25}$$

The effectiveness of the PS wall contribution in the plastic range can be evaluated by considering the total base shear of the system $V_{b,T}$, i.e. the sum of V_{PSW} and $V_{FR,R}$ as in Eq. (26). It can be noted that, while the frame capacity is attained when reaching the capacity in one storey (herein the 1st storey), the capacity increase of the retrofitted system is due to the introduction of the PS wall, and it depends on the capacity of all the storeys and the base equivalent additional resisting moment associated with possible additional devices [expressed as ΔV_d as in Eqs. (26) and (27)].

$$V_{b,T} = V_{FR,R} + \overline{V}_{PSW} + \Delta V_d = \frac{3}{(2n+1)} \sum_{i=1}^{n} \overline{V}_i + \Delta V_d \tag{26}$$

$$\Delta V_d = \frac{3}{(2n+1)} \frac{\overline{M}}{H} \tag{27}$$

As expected, the strength of the retrofitted system is thus not dependent on the storeys lateral stiffness; for this reason, it can be easily estimated once geometry, structural detailing and layout of the existing building are known. Anyway, the ultimate capacity may be impaired by the actual ductility of structural elements. In fact, higher forces are expected to develop in the lower storeys in the case of larger lateral stiffness of the first floor ($\beta \geq 1.5$); this leads to larger displacement and rotation demands, which may trigger a premature activation of plastic hinges, thus requiring more ductility. If the available ductility is not enough to allow for a fully plastic mechanism, the actual capacity of the retrofitted system will be lower than that predicted by the aforementioned equations, which stems as an upper bound reference value. Thus, the proposed analytical approach enables a preliminary evaluation of the eligibility of the existing structures to this kind of retrofit intervention in terms of maximum achievable beneficial effects from a strength point of view. Besides that, the ductility demand in the structural elements before and after the retrofit should be carefully evaluated in order to define the actual effectiveness of the intervention, as for instance by means of a pushover analysis.

As an example, non-linear static analyses were carried out on frames D (Casprini et al. 2019). The analyses were conducted considering a concrete cylindrical strength of 30 MPa, a steel yielding stress of 450 MPa, and the structural details reported in Sect. 3.1 (Table 1). Beam-type elements were used to model both the frame elements and the wall. While the PS wall was modelled as elastic ($E_w = 36{,}283$ MPa, corresponding to C45/55 in EN1992, 2004a), a lumped plasticity approach was adopted to model the frame non-linear behaviour; flexural plastic hinges for beams and columns were defined according to EN1998 (2004b) and moment-axial forces interaction was considered in the definition of column's hinges. Concerning the static loads on the structure, a permanent structural and non-structural load (4 kN/m^2 and 2 kN/m^2, respectively) and a live load of 2 kN/m^2 were considered. Because such frame represents a typical side frame of an existing RC building designed for gravity loading, the loads acting on the beams are relative to an influence area of width 2.5 m. In addition, a linear load of 6 kN/m was included to account for perimetral infills (providing a total of permanent and live load equal to 21 kN/m and 5 kN/m distributed on the beams, respectively) (Casprini et al. 2019). In order to linearize the frame deformation along its height, a value of the wall to frame lateral stiffness χ equal to 0.5 was adopted (by assuming $t_w = 0.25$ m, the length of the wall cross-section L_w is 3.9 m).

Figure 11a and b highlights the role of the PS wall in the retrofit solution through the distribution of plastic hinges at collapse: in the as-is condition (Fig. 11a), the collapse is associated with a soft-storey mechanism at the first level, while the ductility demand spreads along the system after the PS wall introduction (Fig. 11b); in this case, the capacity of the existing structural elements should be verified against the new ductility demand.

The potential benefit of the retrofitted system in terms of maximum achievable strength can be assessed by comparing the capacity of the system before and after the retrofit, similarly to the elastic case. In the as-is condition, the seismic capacity of the system in terms of base shear is herein assumed as the capacity of the 1st storey ($\overline{V}_1$). An additional amplification factor, beyond the elastic field, is easily calculated as the ratio between $V_{b,T}$ and $\overline{V}_1$. If constant shear capacity is assumed in all the storeys, such amplification factor is:

$$\frac{V_{b,T}}{\overline{V}_1} = 3\frac{n\overline{V}_1}{(2n+1)}\frac{1}{\overline{V}_1} = \frac{3n}{2n+1} \tag{28}$$

In this particular case, the increase in capacity depends only on the number of storeys. In real structures, different storey capacities are common. Assuming that the ith storey shear capacity $\overline{V}_i$ uniformly decreases with the height, a parameter $\lambda_i = \overline{V}_i/\overline{V}_{i-1}$ can be defined. Considering a constant mean value of $\lambda_i = \lambda$, the storey shear capacity can be expressed as in Eq. (29), and the new defined amplification factor $V_{b,T}/V_{FR,0}$ ($V_{FR,0} = \overline{V}_1$) depends on the number of storeys and the ratio between different storeys shear capacity; thus an analytical estimate of the number of storeys for which the solution is beneficial can be derived, by imposing that the amplification factor is greater than 1 (Eq. 31). The total base shear of the system can be derived from Eq. (30) as a function of the storey capacity, by neglecting the additional devices contribution for the sake of clarity. When this value is larger than the frame capacity in the as-is condition (Eq. 31), the PS wall provides a potential beneficial effect, that is, an increase in the system strength.

$$\overline{V}_i = \lambda\overline{V}_{i-1} = \overline{V}_1 \cdot \lambda^{i-1} \tag{29}$$

$$V_{b,T} = 3\frac{\sum_{i=1}^{n}\overline{V}_1 \cdot \lambda^{i-1}}{(2n+1)} = 3\frac{\sum_{i=0}^{n-1}\overline{V}_1 \cdot \lambda^{i}}{(2n+1)} = \frac{3\overline{V}_1}{(2n+1)} \cdot \frac{1-\lambda^n}{1-\lambda} \tag{30}$$

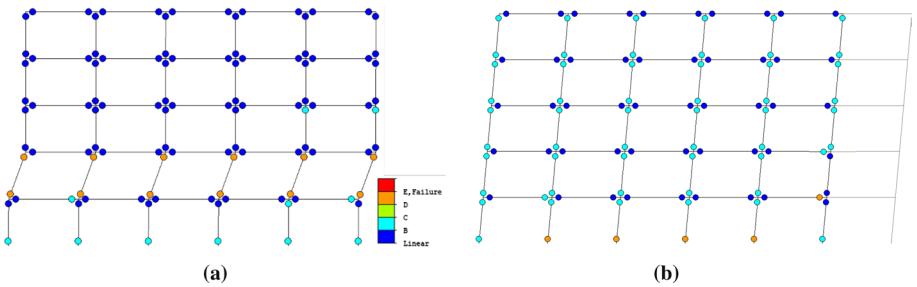

Fig. 11 Comparison of collapse mechanism for Case D in the as-is condition (**a**) and after introducing a PS wall (**b**) with $\chi = 0.5$; capacity curves are reported in Fig. 16

$$\begin{aligned} &\frac{V_{b,T}}{V_{FR,0}} \geq 1 \\ &\frac{V_{b,T}}{V_{FR,0}} = \frac{3}{(2n+1)} \cdot \frac{1-\lambda^n}{1-\lambda} \\ &\frac{1-\lambda^n}{1-\lambda} \geq \frac{(2n+1)}{3} \end{aligned} \tag{31}$$

4.1 Potential benefits of pin-supported walls

In the elastic field the amplification factor was defined as $V_{FR,0}/V_{FR,R}$, i.e. the ratio between the frame base shear before and after the PS wall introduction. This factor depends on β (ratio between the 1st storey lateral stiffness and upper storeys), the number of storeys and the additional contribution provided by possible additional devices. It allows estimating whether the PS wall introduction may reduce the internal action in the frame due to the deformed shape linearization, therefore delaying the onset of yielding. In the case the capacity of the retrofitted system is considered, the amplification factor is defined as $V_{b,T}/V_{FR,0}$ (Eq. 31). Figure 12 shows the application of the analytical formulation for n-storey frames, with n ranging from 2 to 10.

In the case of constant capacity at each floor (i.e. $\lambda = 1$), the same values reported in Fig. 9 are obtained, i.e. the load distribution follows the same pattern in the elastic and inelastic range. The reason of such a result is clarified in Fig. 7, which shows that for a constant storey lateral stiffness the frame story shear is constant after the PS wall introduction, therefore if the lateral capacity is the same in all the storeys, as one storey reaches its capacity, all the others immediately follow leading to the same load amplification of the elastic range. In the case of λ less than 1 a detrimental effect is observed: if each storey shear capacity is equal to 90% ($\lambda = 0.9$), or 80% ($\lambda = 0.8$), of the capacity of the lower storey, the PS wall introduction becomes detrimental for a frame with a number of storeys greater than 8 and 3, respectively. It is worth noting that the coefficient λ for the considered frames (Sect. 3.1) assumes a value of about 0.9 at the 1st storey and ranges within $0.8 \div 0.9$ at the upper storeys. For a deeper understanding of the load distribution as a function of λ,

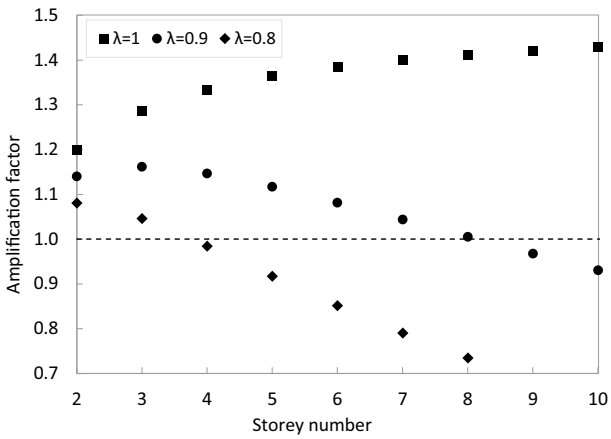

Fig. 12 Amplification factor in a n-storey frame with different storey capacity distribution: constant capacity ($\lambda = 1$), 90% of the lower storey ($\lambda = 0.9$) and 80% of the lower storey ($\lambda = 0.8$)

the behaviour of a 5-story frame is represented in Fig. 13, assuming that the lateral capacity of the 1st storey is 100 and that the capacity of the storeys above are either the same ($\lambda = 1$) (Fig. 13a) or equal to 80% ($\lambda = 0.8$) of the capacity of the storey just below (Fig. 13b). The seismic amplification factor, corresponding to the ratio between the total base shear in the retrofitted case and in the as-is conditions, is equal to 1.36 and 0.91 for the 1st and 2nd case, respectively. For sake of simplicity, the contribution of additional devices was neglected in this example ($\overline{M} = 0$).

It should be noted that, unlike the as-is condition, two aspects are strongly modified after the PS wall introduction: first, the shear distribution in the frame is not decreasing with the height anymore, due to the deformed shape linearization, as seen in the elastic range (Fig. 7); secondly, an increase of the storey shear at the top storey is observed due to deformation compatibility between the frame and the wall. Therefore, when the storey shear capacity is constant, the ultimate capacity is first met in the storey featuring higher internal actions (Fig. 13a), but when the storey capacity decreases according to the height, the top storeys (with a lower capacity) may reach first their ultimate capacity and more load is transferred to the lower storeys, thus reducing the global ultimate capacity (Fig. 13b).

4.2 Sensitivity analysis for non-shear type conditions

The differences between the proposed simplified model and non-shear type conditions in the non-linear range were investigated through a sensitivity analysis. In previous works (Casprini et al. 2019), it was shown that the structural behaviour in the non-linear range is mainly related to the storey nodal ratio (*NR*), herein defined as the mean value of the ratios between the sum of the bending moment capacity of the beams and the sum of the bending moment capacity of the columns converging in each node of a given storey. Such parameter provides an estimation of the strength proportion between columns and beams and consequently the difference from the assumption of strong beams-weak columns. Table 4 reports the results obtained from the sensitivity analysis in terms of a corrective factor for the bending moment in the PS wall (ratio between the real and estimated maximum bending moment) at the system maximum capacity.

It is observed that for a low value of the nodal ratio (i.e. NR = 0.5), the position of the maximum bending moment in the PS wall differs from the one obtained considering a

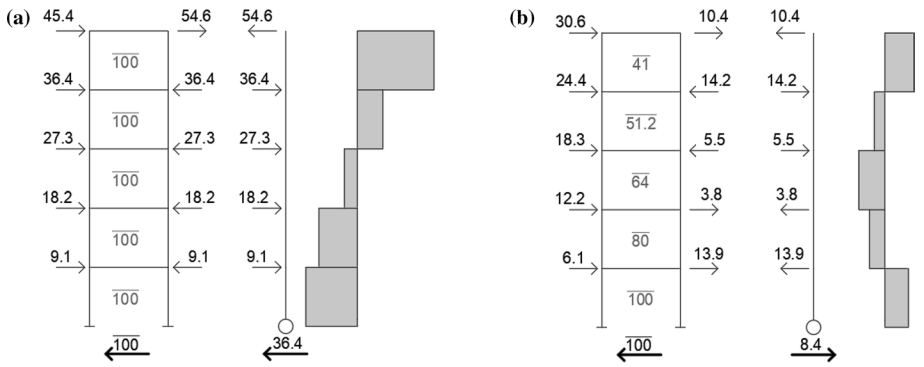

Fig. 13 Load distribution and amplification factor in a 5-storey frame in the case of links at each floor level with different storey capacity distribution: **a** constant ($\lambda = 1$) and **b** 80% ($\lambda = 0.8$) of the lower storey. Note: only one bay of the frame is represented for sake of clarity

shear type behaviour of the frame. This condition is highlighted in Table 4 with a star; although, such difference does not compromise the purpose of the analytical formulation to provide an estimate of the seismic demand on the PS wall.

5 Finite element validation of the proposed procedure

A RC frame was selected to validate the proposed procedure. In particular, the frame referred to as "case D" in Sect. 3.1 was taken into account (main dimensions and structural detailing are reported in Fig. 6, Table 1). The proposed analytical approach is applied following these steps:

- calculation of the PS wall dimensions to linearize the frame deformation along its height;
- calculation of the load distribution in the elastic range;
- calculation of the capacity increase in the inelastic range.

The generic storey lateral stiffness is computed according to Eq. (2), where $H=3$ m is the inter-storey height, considering 6 columns with $k_c=4957$ kNm and 10 beams (5 above and 5 below the storey) with $k_{ga}=k_{gb}=10{,}929$ kNm. The result is $K_s=25{,}680$ kN/m. By selecting a value of $\chi=0.5$, the wall moment of inertia required to linearize the frame deformation is obtained from Eq. (1) with $H_T=15$ m and $E_w=36{,}283$ MPa (C45/55 according to EN1992, 2004a), resulting in $I_w=1.19$ m^4. Consequently, the selected wall length and thickness are $L_w=3.3$ m and $t_w=0.40$ m, respectively. The connecting links are modelled as truss elements with axial stiffness equal to 6300,000 kN/m, corresponding to the axial stiffness of 3 steel plates (300 mm × 300 mm × 10 mm), similarly to the connection investigated in Steele and Wiebe (2020). The storey lateral displacements at yielding are reported in Table 5. The drift concentration factor (DCF) is equal to 3.0 and 1.0 before and after the PS wall introduction; thus, the PS wall introduction is effective in linearizing the lateral deflected shape of the existing frame (Fig. 14).

The load distribution in the frame and in the PS wall can be analytically estimated as proposed in Sect. 3: the coefficient β describing the stiffness increase at the 1st floor was taken equal to 1.29 (obtained from the numerical lateral stiffness estimation in Table 2) and the difference from an ideal shear type behaviour is expressed through the ratio $K_s/K_{S.T}=0.65$. The corrective factor for the maximum bending moment in the PS wall is calculated by interpolating the values reported in Table 3, and it is equal to 1.13. The load

Table 4 Corrective factor for maximum bending moment prediction

NR	λ = 1			λ = 0.9		
	n = 3	n = 5	n = 8	n = 3	n = 5	n = 8
1.5	1.00	1.00	1.00	1.00	0.99	1.00
1.0	1.00	1.00	1.00	0.98	0.99	1.00
0.8	0.76	0.76	0.78	0.77	0.74	0.77
0.5	0.40	0.41	0.46	0.56*	0.54*	0.71*

*The position along the height of the maximum value of the bending moment in the numerical estimate does not correspond to the analytical one

Table 5 Storey lateral displacements before and after the PS wall introduction for top displacement $d_5 = 30$ mm

Storey number	AS-IS		PSW	
	d (mm)	Δ (mm)	$\overline{d}$ (mm)	$\overline{\Delta}$ (mm)
5	30.0	2.7	30.0	5.9
4	27.3	4.9	24.1	5.9
3	22.4	7.0	18.2	6.1
2	15.4	8.2	12.1	6.0
1	7.2	7.2	6.1	6.1
DCF		3.0		1.0

d and Δ are the storey lateral displacement and inter-storey drift, respectively; d and Δ refer to the AS-IS condition while $\overline{d}$ and $\overline{\Delta}$ refer to the retrofitted condition; DCF is the drift concentration factor, i.e. the maximum Δ_j/Δ_j ratio

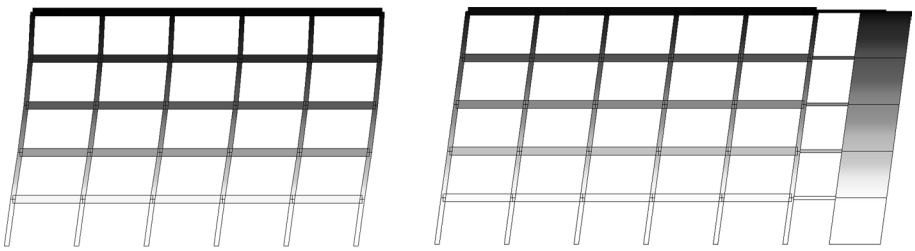

(a) **(b)**

Fig. 14 Deformed shape of frame D at yielding before (**a**) and after (**b**) the PS wall introduction (top displacement equal to 30 mm)

distribution in the system in the elastic range is obtained from Eqs. (10)–(18); a value of αH equal to 13.2 kN (associated with first yielding, that is the STEP Y in the pushover curve of the retrofitted system in Fig. 15a) was taken. The analytical estimation is then compared with the numerical results provided by a linear static analysis carried out with the finite element software MidasGen (2020) (Fig. 15b). The estimated analytical distribution is then adjusted depending on the difference from ideal shear type conditions ("Analytical-adj") by multiplying its values by the aforementioned corrective factor. Figure 15b shows that the results are well predicted by the proposed approach.

Then the system capacity in the nonlinear range is evaluated following the analytical approach presented in Sect. 4, which depends on the storey shear capacity, the number of storeys and the presence of possible additional devices. In order to investigate the effectiveness of the retrofit intervention, the focus was placed on the capacity increase; the capacity of each storey in the frame is computed considering the development of plastic hinges at each column end, considering the column's nominal capacity and accounting for moment-axial load interaction. The beam flexural capacity was not activated due to the weak-column strong-beam characteristic of the frame. The PS wall was modelled as elastic to validate the proposed analytical formulation.

Table 6 reports the storey capacity and the capacity ratio between consecutive storeys ($\lambda_i = \overline{V}_i/\overline{V}_{i-1}$). In the present case study, a reference mean value of $\lambda = 0.9$ was then assumed.

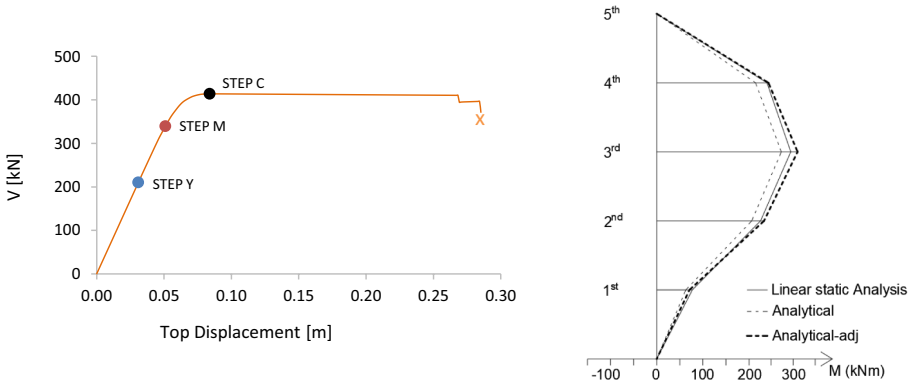

Fig. 15 **a** Pushover curve of the retrofitted system: Y-first yielding ($V_{b,T}$=204 kN); M-maximum bending moment in the PS wall ($V_{b,T}$=340 kN); C-final capacity ($V_{b,T}$=414 kN); **b** PS wall bending moment (M) distribution in the elastic case at STEP Y (αH=13.2 kN) in the case of β=1.29; corrective factor equal to 1.13

The resulting capacity amplification factor is equal to 1.117 (according to Eq. 31), which is in accordance with the results of the pushover curves reported in Fig. 16 (being $V_{FR,0}$=370 kN and $V_{b,T}$=414 kN, the capacity amplification factor is equal to 1.119). If the presence of additional devices is also considered (as a proof of the concept, $\overline{M}$=400 kNm has been selected), the capacity amplification factor obtained from a pushover analysis is equal to 1.241 (in this case $V_{b,T}$=459 kN as represented in Fig. 16 with PSW_$\overline{M}$), while the analytical estimate provides a $V_{b,T}/V_{FR,0}$=1.209 (by calculating $V_{b,T}$=474 kN according to Eq. (26) and assuming $V_{FR,0}=\overline{V}_1$=392 kN from Table 6). For sake of clarity, the results are reported in Table 7.

The maximum bending moment in the PS wall at the system capacity (Fig. 17b) can be estimated through the analytical procedure and then reduced by the proposed corrective factor (Table 4). Considering a mean nodal ratio of 1.27 (Casprini et al. 2019) and λ=0.9, the calculated corrective factor is 0.99, which is rounded to 1. The system capacity estimated by the proposed analytical procedure is 438 kN; this result represents an upper bound prediction of the maximum base shear obtained from the numerical analysis ($V_{b,T}$=414 kN).

It is worth noting that between the first yielding and the attainment of the maximum capacity (step Y and C in Fig. 15a, respectively) a higher value of the bending moment in the PS wall was recorded in the numerical analyses (step M) due to the variation of the load distribution in the connecting links from step Y and step C (Fig. 15a). The proposed simplified model, which well estimates the PS wall demand in the elastic range and after reaching the system capacity, may also be used to provide a rough upper-bound estimate of the maximum bending moment in the PS wall between these two phases. In this regard, the analytical solution for the elastic range may be directly applied by considering the external

Table 6 Storey shear capacity evaluation

STOREY	1	2	3	4	5
$\overline{V}_{STOREY}$ (kN)	392	356	316	272	228
$\lambda_i \times 100(\%)$		91%	89%	86%	84%

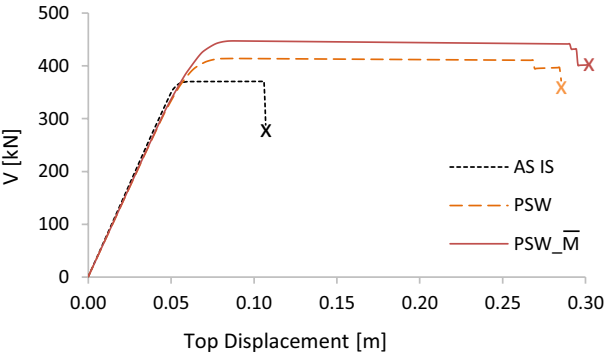

Fig. 16 Pushover curves in the AS-IS condition, after the pin-supported wall introduction (PSW) and with the additional devices (PSW_$\overline{M}$)

Table 7 Comparison between analytical results and FE model analysis

	AS-IS	PSW		PSW_$\overline{M}$			
	$V_{FR,0}$ (kN)	$V_{b,T}$ (kN)	$V_{b,T}/V_{FR,0}$	ΔV_d (kN)	$\Delta V_d/V_{b,T}$ (%)	$V_{b,T}$ (kN)	$V_{b,T}/V_{FR,0}$
Analytical	392	438	1.117	36	7.6	474	1.209
FE analysis	370	414	1.119	45	9.8	459	1.241

load distribution associated with the estimated system capacity (i.e. by considering a strong beam—weak column collapse mechanism and the corrective factor reported in Table 4). The results are summarized in Fig. 17a; however, after the preliminary estimation proposed, the maximum bending moment in the PS wall should be always verified through numerical analysis as the ductility demand in the structural elements of the existing frame. The numerical validation shows that the proposed analytical approach represents a straightforward method for a first estimation of the suitability of PS wall solutions for the retrofit of existing RC frames.

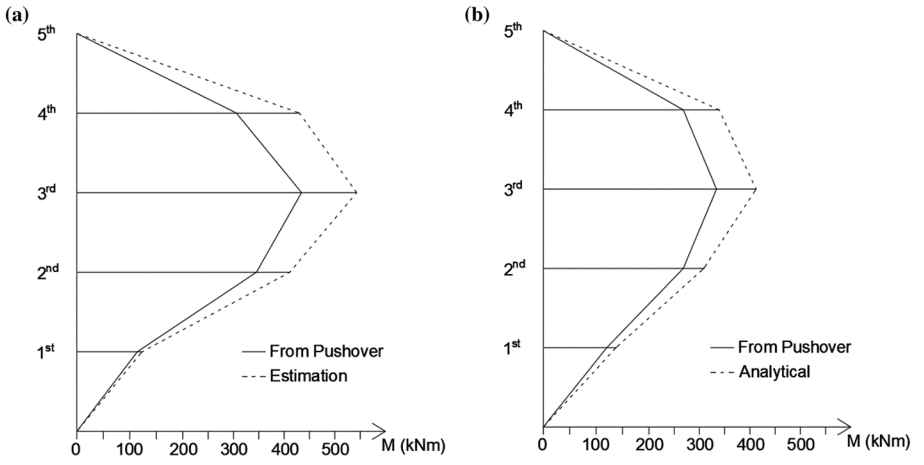

Fig. 17 **a** PS wall maximum bending moment from the pushover analysis (Step M in Fig. 15); **b** PS wall bending moment distribution at system maximum capacity (Step C in Fig. 15) and comparison with the proposed analytical estimation

6 Conclusions

Pin-supported (PS) walls have been used in the last few years as seismic retrofit solutions for existing RC structures; their application allows linearizing the deformation of the frame along its height, thereby avoiding high deformation demand concentrated at one storey. This kind of retrofit intervention does not change the actual capacity of the structural elements at a sectional level, but rather it allows to share the external seismic loading between the frame and the additional walls. Thus, the effectiveness of the solution is strictly related to the ability of well distributing forces among components of the retrofitted system and to the local deformation capacity of the existing structural elements. In the present work, an analytical method to evaluate the potential benefits of this retrofit solution was proposed considering equilibrium equations and enforcing the system deformation compatibility, both in the elastic field and after the storey shear capacity is reached. The method allows to calculate the load distribution in the frame and in the wall introducing either a PS wall connected to the frame at the storey levels by means of truss links or providing additional devices either at the wall-to-frame connections or at the PS wall base. The effect of the storey lateral stiffness was included in the procedure by defining the parameter β, which is the ratio between the 1st storey and the mean intermediate storeys lateral stiffness. It was observed that $\beta \geq 1.5$ may lead to a larger ductility demand on the existing elements, which may compromise the performance of the retrofitted system.

The proposed analytical method was developed on 2D planar models of regular frames retrofitted with the PS wall solution considering the first mode of vibration of the retrofitted system. It is expected that higher modes of vibrations would lead to an increase of the bending moment demand along the PS wall height. However, it is worth mentioning that a possible consequent increase of the PS wall cross-section would not jeopardize the evaluation of the beneficial or detrimental effects of PS wall retrofit solutions derived from the proposed formulation. The method addressed in the paper is based on the assumption of a shear type behaviour of the existing building, which is a reasonable assumption in the case of strong-beams and weak-columns frame systems, although specific corrective factors were provided to derive the maximum bending moment in the PS walls for non-shear type conditions. The analytical formulation and the corrective factors were validated by nonlinear static analyses of a selected case study. It was observed that under some circumstances the adoption of a PS wall may be detrimental, i.e., the base shear of the retrofitted system is lower than that in the as-is conditions; such detrimental effect might be triggered by the progressive reduction of the lateral load capacity of consecutive floors in the existing frame (e.g., a reduction of the storey capacity of 80% between consecutive floors). It is also worth noting that the maximum bending moment in the PS wall may be obtained before reaching the system capacity; a procedure to account for this aspect was also provided.

The proposed approach represents a preliminary tool to evaluate the potential benefits of pin-supported walls as a retrofit solution for existing RC structures and to estimate the pin-supported wall internal actions for a preliminary proportioning also in the case of a coupled system with additional devices. The procedure allows to evaluate such benefits in terms of strength of the retrofitted system. After the beneficial effect has been proved, the ductility demand on the structural elements of the existing frame needs to be assessed, for instance by means of a pushover analysis.

Finally, it must be highlighted that, in seismic retrofitting, a PS wall behaviour could be obtained from downgrading stiff elements of the existing buildings such as the RC stairwell walls.

In future developments, the analytical formulation may include further considerations, such as removing the hypothesis of shear type conditions and assessing the influence of higher modes of vibration. The prediction of the displacement demand may be also analytically investigated, and other failure mechanisms could be considered, along with the 3D configuration of the building. This way, the proposed tool may be used as a preliminary design method, by setting design targets, and consequently defining the characteristics of the dissipative devices.

Appendix 1: Force distribution in the elastic stage

Referring to Fig. 5, the analytical solution of the problem is identified by the following system:

$$\begin{cases} \overline{\Delta_{j+1}} = \overline{\Delta_j} \; j = 1 : n-1 \\ \sum M_0 = 0 \end{cases} \tag{32}$$

$$\overline{\Delta_j} = \frac{\sum_{i=j}^{n} (i\alpha H + N_i)}{K_{s,j}} \tag{33}$$

Condition of equal displacement between consecutive floors (j, j+1) with j varying from 2 and n−1:

$$\overline{\Delta_{j+1}} = \overline{\Delta_j} \rightarrow \frac{\sum_{i=j+1}^{n} (i\alpha H + N_i)}{K_s} = \frac{\sum_{i=j+1}^{n} (i\alpha H + N_i)}{K_s} + \frac{j\alpha H + N_j}{K_s} \tag{34}$$

$$\frac{j\alpha H + N_j}{K_s} = 0 \rightarrow N_j = -j\alpha H \text{ for } j = 2 : n-1 \tag{35}$$

To obtain N_1 and N_n, the condition of equal displacements of the first and second storey and the equilibrium of forces with respect to the rotation at the base of the pin-supported wall are considered.

$$\begin{cases} \overline{\Delta_2} = \overline{\Delta_1} \\ \sum M_0 = 0 \end{cases} \rightarrow \begin{cases} \frac{\sum_{i=2}^{n} i\alpha H + N_i}{K_s} = \frac{\sum_{i=1}^{n} i\alpha H + N_i}{\beta K_s} \\ N_1 H - \alpha H^2 \sum_{i=2}^{n-1} i^2 + N_n n H + \overline{M} = 0 \end{cases} \tag{36}$$

From the first equation of the system and the value of N_j an expression of N_1 is obtained:

$$\frac{n\alpha H + N_n}{K_s} = \frac{\alpha H + N_1 + n\alpha H + N_n}{\beta K_s} \rightarrow \beta(n\alpha H + N_n) = \alpha H + N_1 + n\alpha H + N_n \tag{37}$$

$$N_1 = (\beta - 1)(n\alpha H + N_n) - \alpha H \tag{38}$$

Considering the second equation of the system (36), in general:

$$\sum_{k=1}^{n} k^2 = \frac{n(n+1)(2n+1)}{6} \rightarrow \sum_{i=2}^{n-1} i^2 = \frac{n(n+1)(2n+1)}{6} - 1 - n^2 = \frac{2n^3 - 3n^2 + n - 6}{6} \tag{39}$$

By substituting (39) in (36), N_n can be defined:

$$\begin{aligned}
&(\beta - 1)(n\alpha H + N_n)H - \alpha H^2 - \alpha H^2 \frac{2n^3 - 3n^2 + n - 6}{6} + N_n nH + \overline{M} = 0 \\
&(\beta - 1)(n\alpha H + N_n) - \alpha H - \alpha H \frac{2n^3 - 3n^2 + n - 6}{6} + N_n n + \frac{\overline{M}}{H} = 0 \\
&N_n(n + \beta - 1) = \frac{\alpha H}{6}(2n^3 - 3n^2 + n - 6 + 6n - 6n\beta + 6) - \frac{\overline{M}}{H} \\
&N_n(n + \beta - 1) = \frac{\alpha H}{6}(2n^3 - 3n^2 + 7n - 6n\beta) - \frac{\overline{M}}{H} \\
&N_n = \left[\frac{n\alpha H}{6}(2n^2 - 3n + 7 - 6\beta) - \frac{\overline{M}}{H}\right]\frac{1}{(n + \beta - 1)} \\
&N_n = \frac{\alpha H}{6}\frac{(2n^3 - 3n^2 + 7n - 6\beta n) - \frac{6\overline{M}}{\alpha H^2}}{(n + \beta - 1)}
\end{aligned} \tag{40}$$

Starting from the expression of N_1 (38) and substituting the value of N_n (40):

$$N_1 = -\alpha H + n\alpha H\beta - n\alpha H + N_n\beta - N_n \tag{41}$$

$$N_1 = \alpha H(n\beta - 1 - n) + (\beta - 1)N_n$$

$$N_1 = \alpha H(n\beta - 1 - n) + (\beta - 1)\frac{\alpha H}{6}\frac{2n^3 - 3n^2 + 7n - 6\beta n - \frac{6\overline{M}}{\alpha H^2}}{n + \beta - 1}$$

$$N_1 = \frac{\alpha H}{6}\frac{\left[6(n + \beta - 1)(n\beta - 1 - n) + (\beta - 1)(2n^3 - 3n^2 + 7n - 6\beta n - \frac{6\overline{M}}{\alpha H^2})\right]}{n + \beta - 1}$$

$$N_1 = \frac{\alpha H}{6}\frac{(2n^3 + 3n^2 - 6)(\beta - 1) + n(\beta - 7) + \frac{6\overline{M}}{\alpha H^2}(1 - \beta)}{n + \beta - 1} \tag{42}$$

The equation of the base shear both for the pin-supported wall and for the frame is provided:

$$V_{PSW} = -\sum_{i=1}^{n} N_i = -N_1 - N_n + \alpha H \sum_{i=2}^{n-1} i \tag{43}$$

$$N_1 + N_n = \frac{\alpha H}{6} \frac{2\beta n^3 + 3\beta n^2 - 6n^2 - 6\beta + 6 - 5\beta n - 7n - \frac{6\overline{M}}{\alpha H^2}\beta}{n + \beta - 1}$$

$$V_{PSW} = -\frac{\alpha H}{6} \frac{2\beta n^3 + 3\beta n^2 - 6n^2 - 6\beta + 6 - 5\beta n - 7n - \frac{6\overline{M}}{\alpha H^2}\beta}{n + \beta - 1} + \alpha H \frac{n^2 - n - 2}{2}$$

$$V_{PSW} = \frac{\alpha H}{6} \frac{(n^3 - n)(3 - 2\beta) + \frac{6\overline{M}}{\alpha H^2}\beta}{n + \beta - 1} \tag{44}$$

The frame base shear can be obtained as the difference between the total external forces and the shear at the pin-supported wall base:

$$V_{FR,R} = \alpha H \sum_{i=1}^{n} i - V_{PSW} \tag{45}$$

$$V_{FR,R} = \alpha H \frac{n^2 + n}{2} - V_{PSW}$$

$$V_{FR,R} = \frac{\alpha H}{6} \frac{3n^3 + 3\beta n^2 + 3\beta n - 3n - 3n^3 + 2\beta n^3 - 2\beta n + 3n - \frac{6\overline{M}}{\alpha H^2}\beta}{n + \beta - 1}$$

$$V_{FR,R} = \frac{\alpha H}{6} \frac{n\beta(2n^2 + 3n + 1) - \frac{6\overline{M}}{\alpha H^2}\beta}{n + \beta - 1} \tag{46}$$

Appendix 2: Force distribution beyond the elastic stage

Referring to Fig. 10, the analytical solution of the problem is identified by the following system:

$$\begin{cases} N_n + n(\alpha H + \delta_F) = \overline{V}_n & j = n \\ N_j + j(\alpha H + \delta_F) + \overline{V}_{j+1} = \overline{V}_j & j = 1 : n-1 \\ \sum_{i=1}^{n} N_i i H + \overline{M} = 0 \end{cases} \tag{47}$$

By taking into account the equilibrium equation at each floor level, an explicit expression of each storey can be obtained, which is different only for the upper floor level:

$$N_n = \overline{V}_n - n(\alpha H + \delta_F) \tag{48}$$

$$N_i = \overline{V}_i - \overline{V}_{i+1} - i(\alpha H + \delta_F) \tag{49}$$

The equilibrium of forces with respect to rotation for the pin-supported wall can be written as:

$$\sum_{i=1}^{n-1} N_i i + N_n n + \frac{\overline{M}}{H} = 0 \tag{50}$$

$$\sum_{i=1}^{n-1} \left[i(\overline{V}_i - \overline{V}_{i+1}) - i^2(\alpha H + \delta_F) \right] + \frac{\overline{M}}{H} = -n\left[\overline{V}_n - n(\alpha H + \delta_F) \right]$$

$$\sum_{i=1}^{n-1} i(\overline{V}_i - \overline{V}_{i+1}) - (\alpha H + \delta_F) \sum_{i=1}^{n-1} i^2 + \frac{\overline{M}}{H} = -n\left[\overline{V}_n - n(\alpha H + \delta_F) \right]$$

By considering that:

$$\sum_{i=1}^{n-1} i(\overline{V}_i - \overline{V}_{i+1}) = \sum_{i=1}^{n} \overline{V}_i - n\overline{V}_n$$

The equation becomes:

$$\sum_{i=1}^{n} \overline{V}_i - n\overline{V}_n - (\alpha H + \delta_F) \sum_{i=1}^{n-1} i^2 + \frac{\overline{M}}{H} = -n\overline{V}_n + n^2(\alpha H + \delta_F)$$

$$\sum_{i=1}^{n} \overline{V}_i - (\alpha H + \delta_F) \sum_{i=1}^{n} i^2 + \frac{\overline{M}}{H} = 0$$

$$(\alpha H + \delta_F) = \frac{\sum_{i=1}^{n} \bar{V}_i + \frac{\overline{M}}{H}}{\sum_{i=1}^{n} i^2}$$

Given that:

$$\sum_{i=1}^{n} i^2 = \frac{n(n+1)(2n+1)}{6}$$

$$(\alpha H + \delta_F) = 6\frac{\sum_{i=1}^{n} \bar{V}_i + \frac{\overline{M}}{H}}{n(n+1)(2n+1)} \tag{51}$$

$$N_n = \overline{V}_n - 6\frac{\sum_{i=1}^{n} \bar{V}_i + \frac{\overline{M}}{H}}{(n+1)(2n+1)} \tag{52}$$

$$N_i = \overline{V}_i - \overline{V}_{i+1} - 6i\frac{\sum_{i=1}^{n}\bar{V}_i + \frac{\overline{M}}{H}}{n(n+1)(2n+1)} \tag{53}$$

The equation of the base shear both for the pin-supported wall and for the frame is provided:

$$V_{PSW} = -\sum_{i=1}^{n} N_i = -N_n - \sum_{i=1}^{n-1} N_i \tag{54}$$

$$V_{PSW} = -\left[\overline{V}_n - 6\frac{\sum_{i=1}^{n}\bar{V}_i + \frac{\overline{M}}{H}}{(n+1)(2n+1)} + \sum_{i=1}^{n-1}(V_i - V_{i+1}) - \frac{6}{n}\frac{\sum_{i=1}^{n}\bar{V}_i + \frac{\overline{M}}{H}}{(n+1)(2n+1)}\sum_{i=1}^{n-1} i\right]$$

$$V_{PSW} = -\left[\overline{V}_1 - 6\frac{\sum_{i=1}^{n}\bar{V}_i + \frac{\overline{M}}{H}}{(n+1)(2n+1)}(1 + \frac{n^2-n}{2n})\right]$$

$$V_{PSW} = 3(n+1)\frac{\sum_{i=1}^{n}\bar{V}_i + \frac{\overline{M}}{H}}{(n+1)(2n+1)} - \overline{V}_1$$

$$V_{PSW} = 3\frac{\sum_{i=1}^{n}\bar{V}_i + \frac{\overline{M}}{H}}{(2n+1)} - \overline{V}_1 \tag{55}$$

The frame base shear can be obtained as the difference between the total seismic forces and the shear at the pin-supported wall base:

$$V_{FR,R} = (\alpha H + \delta_F)\sum_{i=1}^{n} i - V_{PSW} \tag{56}$$

$$V_{FR,R} = 6\frac{\sum_{i=1}^{n}\bar{V}_i + \frac{\overline{M}}{H}}{n(n+1)(2n+1)}\frac{n(n+1)}{2} - 3\frac{\sum_{i=1}^{n}\bar{V}_i + \frac{\overline{M}}{H}}{(2n+1)} + \overline{V}_1$$

$$V_{FR,R} = \overline{V}_1 \tag{57}$$

Funding No specific funding was assigned to this research.

Data availability The raw data supporting the conclusions of this article will be made available by the authors, upon reasonable requests.

Code availability Closed-source software was employed.

Declarations

Conflict of interest The authors declare that the research was conducted in the absence of any commercial or financial relationships that could be construed as a potential conflict of interest.

References

Balducci A, Castellano MG (2015) Seismic retrofitting of a RC school building through the "Damping Towers" system. Progettazione Sismica 6(1):69–91. https://doi.org/10.7414/PS.6.1.69-91 (**in Italian**)

Belleri A, Marini A (2016) Does seismic risk affect the environmental impact of existing buildings? Energy Build 110(1):149–158. https://doi.org/10.1016/j.enbuild.2015.10.048

Belleri A, Passoni C, Marini A, Riva P (2016) Hinged-wall solutions for the structural strengthening of existing RC buildings. Fib Symposium 2016, Cape Town, South Africa, 21–23 November 2016

Blebo FC, Roke DA (2015) Seismic-resistant self-centering rocking core system. Eng Struct 101:193–204. https://doi.org/10.1016/j.engstruct.2015.07.016

Bozdogan KB, Öztürk D (2016) A method for dynamic analysis of frame-hinged shear wall structure. Earthq Struct 11(1):45–61. https://doi.org/10.12989/eas.2016.11.1.045

Casprini E, Belleri A, Passoni C, Labò S, Marini A (2019) Computational issues of hinged walls used as retrofitting of existing frames. Eccomas Proceedia COMPDYN 2019:3006–3018. https://doi.org/10.7712/120119.7128.19126

EN 1992 (2004a) Eurocode 2: design of concrete structures. CEN, Brussels

EN 1998 (2004b) Eurocode 8: design of structures for earthquake resistance. CEN, Brussels

Feroldi F, Marini A, Badiani B, Plizzari G, Giuriani E, Riva P, Belleri A (2013) Energy efficiency upgrading, architectural restyling and structural retrofit of modern buildings by means of "engineered" double skin façade. International Conference on Structures and Architecture, Guimaraes, Portugal, 24–26/07/2013. ISBN 978-0-415-66195-9, pp 1859–1866

Gioiella L, Balducci A, Carbonari S, Gara F, Dezi L (2017) An innovative seismic protection system for existing buildings: external dissipative towers. In: 16th World Conference on Earthquake Engineering 16WCEE 2017, Santiago, Chile

Labò S, Passoni C, Marini A, Belleri A, Camata G, Riva P, Spacone E (2017) Prefabricated responsive diagrids for holistic renovation of existing MID-RISE RC buildings. In: Proceedings of the 6th International Conference on Computational Methods in Structural Dynamics and Earthquake Engineering COMPDYN 2017, vol 2, pp 4234–4244

MacRae G, Kimura Y, Roeder C (2004) Effect of column stiffness on braced frame seismic behavior. J Struct Eng 130(3):381–391. https://doi.org/10.1061/(ASCE)0733-9445(2004)130:3(381)

Marini A, Passoni C, Belleri A, Feroldi F, Metelli G, Preti M, Giuriani E, Riva P, Plizzari G (2017) Combining seismic retrofit with energy refurbishment for the sustainable renovation of RC buildings: a proof of concept. Eur J Environ Civ Eng 10:1080

Midas GEN, Analysis manual for Midas GEN; release 2020

Pan P, Wu S, Nie X (2015) A distributed parameter model of a frame pin-supported wall structure. Earthq Eng Struct Dynam 44(10):1643–1659. https://doi.org/10.1002/eqe.2550

Qu Z, Wada A, Motoyui S, Sakata H, Kishiki S (2012) Pin-supported walls for enhancing the seismic performance of buildings structures. Earthq Eng Struct Dynam 41(14):2075–2091. https://doi.org/10.1002/eqe.2175

Qu Z, Sakata H, Midorikawa S, Wada A (2015a) Lessons from the behavior of a monitored 11-story building during the 2011 Tohoku earthquake for robustness against design uncertainties. Earthq Spectra 31(3):1471–1492. https://doi.org/10.1193/051813EQS126M

Qu B, Sanchez-Zamora F, Pollino M (2015b) Transforming seismic performance of deficient steel concentrically braced frames through implementation of rocking cores. J Struct Eng 141(5):04014139. https://doi.org/10.1061/(ASCE)ST.1943-541X.0001085

Rahgozar N, Rahgozar N (2020) Extension of direct displacement-based design for quantifying higher mode effects on controlled rocking steel cores. Struct Design Tall Spec Build 29:e1800. https://doi.org/10.1002/tal.1800

Rahgozar N, Moghadam AS, Aziminejad A (2018) Continuum analysis approach for rocking core-moment frames. J Struct Eng 144(3):0001986. https://doi.org/10.1061/(ASCE)ST.1943-541X.0001986
Schultz AE (1992) Approximating lateral stiffness of stories in elastic frames. J Struct Eng 118(1):243–263
Steele TC, Wiebe LDA (2020) Large-scale experimental testing and numerical modeling of floor-to-frame connections for controlled rocking steel braced frames. J Struct Eng 146(8):0002722. https://doi.org/10.1061/(ASCE)ST.1943-541X.0002722
Sullivan TJ, Priestley MJN, Calvi GM (2008) Estimating the higher-mode response of ductile structures. J Earthq Eng 12(3):456–472
Sun T, Kurama YC, Zhang P, Ou J (2017) Linear-elastic lateral load analysis and seismic design of pin-supported wall-frame structures with yielding dampers. Earthq Eng Struct Dynam 47(4):988–1013. https://doi.org/10.1002/eqe.3002
Wada A (2018) Strength, functionality and beauty of university buildings in earthquake-prone countries. Proc Jpn Acad Ser B 94:129–138
Wada A, Qu Z, Ito H, Motoyui S, Sakata H, Kasai K (2009) Seismic retrofit using rocking walls and steel dampers. In: ATC/SEI Conference on improving the Seismic Performance of Existing Buildings and Other Structures, San Francisco, CA, U.S, Dec 2009
Wada A, Qu Z, Motoyui S, Sakata H (2011) Seismic retrofit of existing SRC frames using rocking walls and steel dampers. Front Architect Civil Eng China 5(3):259–266. https://doi.org/10.1007/s11709-011-0114-x
Wiebe L, Christopoulos C (2015) A cantilever beam analogy for quantifying higher mode effects in multi-storey buildings. Earthq Eng Struct Dynam 44(11):1697–1716
Zhou Y, Yao D, Chen Y, Li Q (2021) Upgraded parameter model of frame pin-supported wall structures. Struct Design Tall Spec Build 30:e1852. https://doi.org/10.1002/tal.1852

Authors and Affiliations

Elena Casprini[1] · Andrea Belleri[1] · Alessandra Marini[1] · Simone Labò[1] · Chiara Passoni[1]

Elena Casprini
elena.casprini@unibg.it

Alessandra Marini
alessandra.marini@unibg.it

Simone Labò
simone.labo@unibg.it

Chiara Passoni
chiara.passoni@unibg.it

[1] Department of Engineering and Applied Sciences, University of Bergamo, Viale Marconi 5, 24044 Dalmine, Italy